

1992

Characterization of Thermal Processes in Scroll Compressors

T. C. Wagner

United Technologies Research Center

A. J. Marchese

United Technologies Research Center

D. J. McFarlin

United Technologies Research Center

Follow this and additional works at: <https://docs.lib.purdue.edu/icec>

Wagner, T. C.; Marchese, A. J.; and McFarlin, D. J., "Characterization of Thermal Processes in Scroll Compressors" (1992).
International Compressor Engineering Conference. Paper 796.
<https://docs.lib.purdue.edu/icec/796>

This document has been made available through Purdue e-Pubs, a service of the Purdue University Libraries. Please contact epubs@purdue.edu for additional information.

Complete proceedings may be acquired in print and on CD-ROM directly from the Ray W. Herrick Laboratories at <https://engineering.purdue.edu/Herrick/Events/orderlit.html>

CHARACTERIZATION OF THERMAL PROCESSES IN SCROLL COMPRESSORS

T. C. Wagner
Associate Research Engineer
(203) 727-7589

A. J. Marchese
Assistant Research Engineer
(203) 727-7785

D. J. McFarlin
Manager, Advanced Compressor Technology
(203) 727-7432

United Technologies Research Center
Silver Lane - M.S. 19
East Hartford, CT 06108
FAX (203) 727-7656

ABSTRACT

The efficiency of vapor compressors is strongly affected by the heat transfer occurring both internal and external to the compressor. An experimental investigation was conducted to characterize the thermal processes in scroll compressors. Of special interest was the distribution of the heat generated inside the shell, some of which is absorbed by the suction gas while the remainder is rejected to the surroundings. The investigation included temperature, pressure and heat flux measurements from several prototype scroll compressors operating over the full range of expected conditions. Temperature, obtained from thermocouples, an optical pyrometer, or liquid crystal coatings, was measured at several locations both inside and on the external surface of the shell. Heat flux gauges were used to measure the heat flux on the shell and at locations inside the shell. A description of an analytical model currently under development is also presented.

NOMENCLATURE

Symbols

\dot{E}_{in} total compressor input power
h enthalpy per unit mass
 \dot{m} mass flow rate
P pressure
q heat flux
 \dot{Q} heat transfer rate
V volume
 \dot{W}_s shaft power

Subscripts

b bearings
sep separator plate
dome shell discharge region
m motor
out total compressor shell
pri primary flow path
P scroll elements
sec secondary flow path
shell shell suction region
tube discharge tube
1 inlet to compressor shell
2 inlet to scroll elements
5 discharge from scroll elements
7 exit from compressor shell

INTRODUCTION

Scroll compressors have received the attention of the HVAC industry because of their high efficiency, reliability, low noise and minimal vibration. While these benefits are characteristic of the scroll design, additional research will yield improved performance. A major factor which significantly impacts performance is the heat transfer occurring both inside and on the shell of the compressor. These thermal processes are important to compressor efficiency because they affect the mass flow rate and compressor power, which for a given condition completely determine the compressor performance. In a displacement compressor with a given rate of leakage, volume flow rate is fixed, resulting in a mass flow rate which is directly proportional to the density of the suction gas at the start of compression. Therefore, compressor efficiency is proportional to the density at the start of compression divided by the total input power.

Heat transfer processes affect both power and suction gas density in several ways:

- 1) motor efficiency decreases with increasing temperature due to the increase in motor winding resistance,
- 2) indicated PV power required for gas compression is a strong function of the heat flux to the scroll compressor elements, and,
- 3) any temperature rise in the suction gas from the time it enters the compressor shell until the start of closed compression results in decreased gas density.

In hermetic compressors where it is necessary to use the suction gas to cool the motor and the oil, the thermal processes must be well understood in order to maximize efficiency. Accordingly, an experimental investigation was conducted to characterize internal and external compressor temperatures and heat fluxes over a range of operating conditions. An analytical model incorporating the underlying convection, conduction and radiation processes is currently under development.

EXPERIMENTAL PROCEDURE

Laboratory Test Compressors

In order to experimentally determine the shell flow and heat transfer characteristics, several SC-37 (37,000 Btu/hr) Carrier low-side scroll compressors were installed into bolted shells that were fitted with an instrumentation ring to facilitate feeding the instrumentation cabling out of the compressor. These instrumented scroll compressors thus differed from welded shell, hermetic scroll compressors in several ways:

- 1) The instrumentation ring increased the overall area of the compressor shell exposed to ambient air;
- 2) The instrumentation ring increased the volume of the refrigerant gas between the fixed scroll and the underside of the discharge dome separator plate; and,
- 3) the bolted shell decreased heat conduction paths within the compressor shell.

These differences are expected to have only a minor effect on the characteristics of the compressor. Therefore, the understanding gained from this investigation will be applicable to hermetic scroll compressors. Figure 1 is a photograph of one of the laboratory test compressors in test configuration.

Instrumentation and Data Acquisition

To perform these tests, laboratory scroll compressor "A" was instrumented with 6 heat flux gauges and 37 thermocouples. The 37 thermocouples were installed to measure the following:

- o upper and lower journal bearing temperatures,
- o motor temperatures,
- o internal shell gas temperatures,
- o suction gas temperature rise in the suction ducting,
- o total suction gas temperature rise,
- o external shell temperature profiles,
- o fixed scroll temperature profiles,
- o oil temperatures, and
- o discharge plenum temperatures.

The heat flux gauges were installed to measure:

- o discharge dome heat flux,
- o center shell heat flux,
- o oil sump heat flux,
- o fixed scroll heat flux, and
- o discharge dome separator plate heat flux.

Laboratory scroll compressor "B" was instrumented with 6 heat flux gauges and 28 thermocouples to measure most of the above parameters. In addition, a portion of compressor B was painted with temperature sensitive liquid crystal paint to determine temperature gradients on the compressor shell in the vicinity of the suction line connection. A mixture of 4 paints was used, providing visible transitions in color at 90F, 100F, 112F and 130F. The shell temperature gradients were further validated using an infrared pyrometer. The pyrometer was calibrated by changing its emissivity adjustment until the pyrometer readout matched the temperature as indicated by a thermocouple on the compressor shell. The calibration was checked against several thermocouples on the compressor and found to be accurate. (The emissivity of the black paint on the shell was 0.92.)

The data were acquired, stored, reduced, displayed, and plotted using the laboratory data system at United Technologies Research Center (UTRC) [ref 1]. A schematic diagram of one of the laboratory scroll compressors integrated with the data system is shown in Figure 2. In addition, a stand-alone computer and data logger were used to acquire heat flux data.

Test Procedure

The laboratory test compressors were tested on desuperheater and calorimeter test stands equipped with suction and discharge pressure transducers and thermocouples to accurately determine operating conditions. Each test stand was charged with R22 and tested at up to 22 operating conditions. Each condition had 20 degrees suction superheat.

EXPERIMENTAL RESULTS

Shell Temperature Profiles

Circumferential temperature measurements are presented in Fig. 3 for the "B" compressor operating at the 45/130 condition (45F = saturated evaporating temperature, 130F = saturated condensing temperature). The measured temperatures are normalized by the maximum shell temperature. The temperature distributions in the sump, motor and discharge planes are fairly uniform over the circumference. The suction plane and instrumentation ring distributions are uniform over 75 percent of the circumference, but exhibit lower temperatures in the suction region. The lowest temperatures on the shell were on the instrumentation ring.

For most tests, the temperature profiles were recorded for two angular locations - 0 degrees (in line with the suction duct) and 180 degrees (opposite the suction duct). The circumferential measurements of Fig. 3 were used to develop weighting factors so that the temperature profiles could be averaged. The average temperature profiles of five different operating conditions are compared in Fig. 4. The temperature profiles are seen to have a maximum on the top of the discharge dome and a minimum in the region near the suction duct. The shell temperatures near the oil sump and motor are nearly uniform and are approximately 85 percent of the peak temperature in four of the five cases. The 45/90 case has a shell temperature in the motor region which differs by only 2 percent from the dome temperature. This uniformity is the result of the lower discharge temperature and lower loads which generate less waste heat at this condition.

Temperature contours in the region of the suction entrance are shown in Fig. 5 for 4 saturated condensing temperatures. These contours were obtained from photographs of the liquid crystal paint. The region near the suction connection is black, indicating a temperature less than the lowest transition of the liquid crystal paint (90F). This region is cooled by the suction gas, which is directed vertically upward along the inside of the shell. The spacing of the contours is seen to decrease with increasing saturated condensing temperature, indicating an increase in heat flux to the suction gas.

Heat Flux Results

The shell heat flux data are presented in Fig. 6. These data were corrected for emissivity differences between the heat flux gauges and the black paint on the shell. The energy dissipated through radiative exchange with the surroundings was approximately equal to the energy dissipated through convection. The largest flux occurs on the dome, corresponding to the region of maximum surface temperature. The heat flux data were used to demonstrate a global energy balance to within 2 percent of the input power.

Heat flux data were also used to verify previous assumptions regarding the absorption of waste heat by the suction gas. Current simulation models used to calculate suction superheat temperature require as input the proportion of mechanical and electrical losses which are absorbed by the suction gas. The remaining waste heat is assumed to be dissipated by radiation and convection to the surroundings. The heat flux data and suction gas temperature measurements were useful in verifying that approximately 80 percent of the waste heat is absorbed by the suction gas for this suction duct arrangement.

The heat fluxes from the fixed scroll and the discharge plenum separator plate are presented in Fig. 7. The separator plate heat flux is seen to increase with increasing saturated condensing temperature, while the scroll heat flux is uniform over most of the range tested. These results indicate that separator plate heat flux is dominated by discharge temperature and the heat leaving the scrolls is primarily the result of friction.

Effect of Operating Condition on Thermal Characteristics

The variety of operating conditions required in air conditioning and heat pump applications results in a wide range of compressor operating parameters such as motor torque and mass flow rate. In order to fully understand the effect of these varying parameters on compressor heat transfer processes, scroll compressor A was tested at 22 operating conditions, corresponding to the range of saturated evaporating temperatures and saturated condensing temperatures typically encountered. Data were acquired from the 37 thermocouples and 6 heat flux gauges. Contour plots of the representative temperature and heat flux data are included in the following figures:

<u>Figure</u>	<u>Contour Plot</u>
8	Suction Duct Temperature Rise
9	Total Suction Gas Temperature Rise
10	Oil Temperature
11	Main Bearing Temperature
12	Discharge Temperature
13	Center Shell Heat Flux

For each of these plots, the contours were normalized with respect to the maximum measured value of that parameter during the 22 test conditions.

ANALYTICAL MODEL DEVELOPMENT

An analytical model is currently being developed to provide a tool for understanding and improving the thermal processes in scroll compressors. The schematic diagram of the system on which the model is based is shown in Fig. 14. The global energy balance for this system is

$$\frac{\dot{E}_{in} - \dot{Q}_{out}}{m} = h_7 - h_1. \quad (1)$$

The heat leaving the system is

$$\dot{Q}_{out} = \dot{Q}_{shell} + \dot{Q}_{dome} + \dot{Q}_{tube}. \quad (2)$$

The change in enthalpy may be expressed in increments:

$$\Delta h_{7-1} = \Delta h_{7-5} + \Delta h_{5-2} + \Delta h_{2-1} \quad (3)$$

where: $\Delta h_{2-1} = (\dot{Q}_{pri} + \dot{Q}_{sec}) / \dot{m}$ (4)

$$= (\dot{m}_{pri} \Delta h_{pri,2-1} + \dot{m}_{sec} \Delta h_{sec,2-1}) / \dot{m}$$

$$\Delta h_{5-2} = (\dot{W}_s - \dot{Q}_p) / \dot{m} \quad (5)$$

$$\Delta h_{7-5} = -(\dot{Q}_{dome} + \dot{Q}_{disc} + \dot{Q}_{tube}) / \dot{m}. \quad (6)$$

These incremental enthalpy changes are the result of heat transfer to and work done on the refrigerant. Each term in these equations may be modelled separately. For example, the heat transfer to the secondary path, \dot{Q}_{sec} , may be modelled as a convective heat transfer process where the secondary flow, \dot{m}_{sec} , absorbs waste heat from the motor and bearings. Heat generated by the motor may be determined from motor efficiency data, and a journal bearing code which was developed at UTRC may be used to determine the heat generated by the bearings. The heat transfer coefficient may be determined from experimental data or published correlations. The flow rate through the secondary path depends on the geometry of the internal suction ducting.

Once the individual models are completed, they will be incorporated into a global heat transfer model which will be used to predict steady state compressor operating parameters such as suction superheat temperature (T_2), discharge temperature (T_7), and mass flow rate (\dot{m}). The global model will not require any assumptions as to the proportion of waste heat absorbed by the suction gas. Rather, the physical models contained therein will be sufficient to predict this behavior.

SUMMARY

Thermal characteristics of a scroll compressor were experimentally determined over a wide range of operating conditions. These characteristics include heat flux data, internal gas and component temperatures, and shell temperature distributions. Heat flux and temperature data were used to verify the proportion of waste heat absorbed by the suction gas. A description was given of an analytical model which is currently under development.

REFERENCE

1. Marchese, A. J., "Dynamics of an Orbiting Scroll with Axial Compliance - Part 1: Experimental Techniques", Proceedings of the 1992 International Compressor Engineering Conference at Purdue.

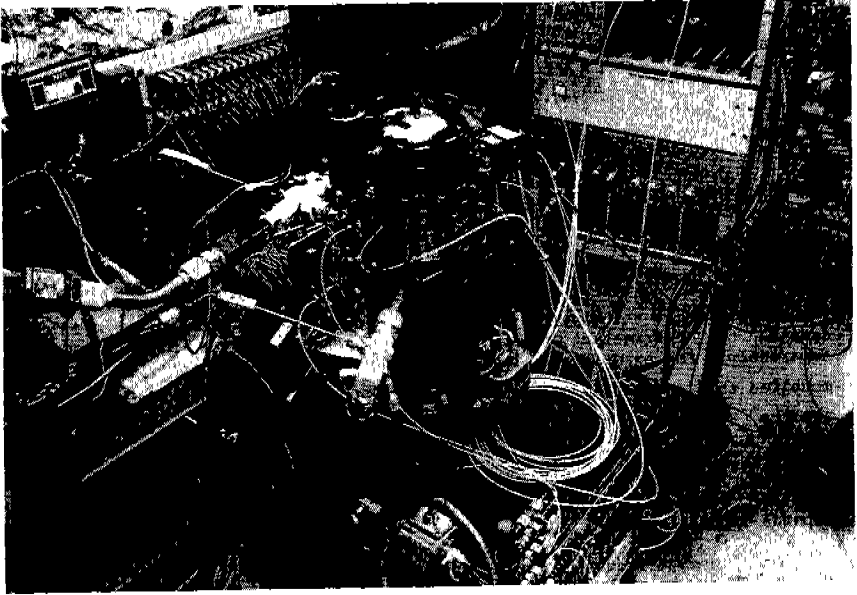


Fig. 1. Laboratory test compressor in test configuration

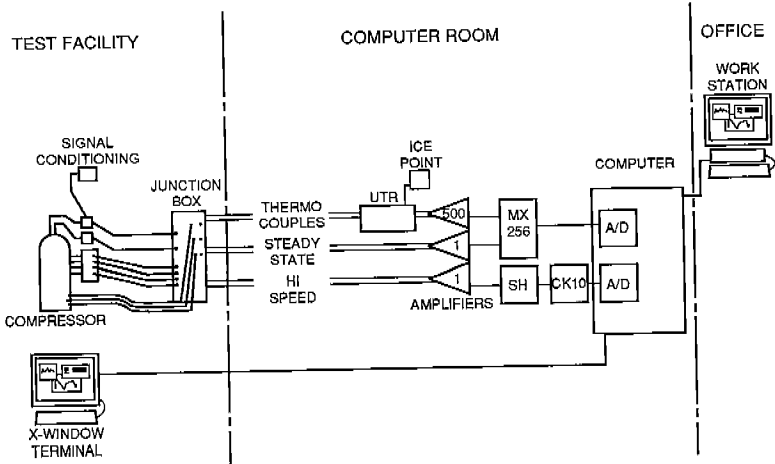


Fig. 2. Laboratory data system

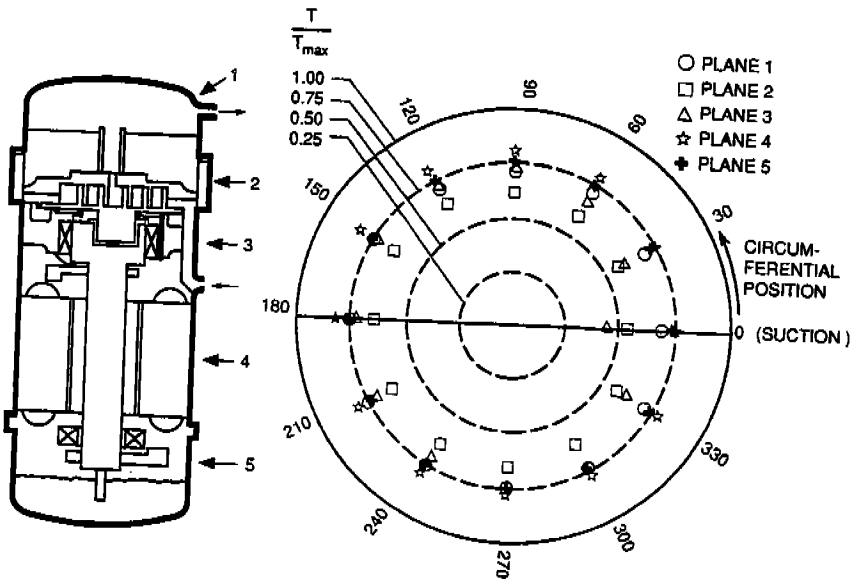


Fig. 3. Circumferential shell temperature profiles

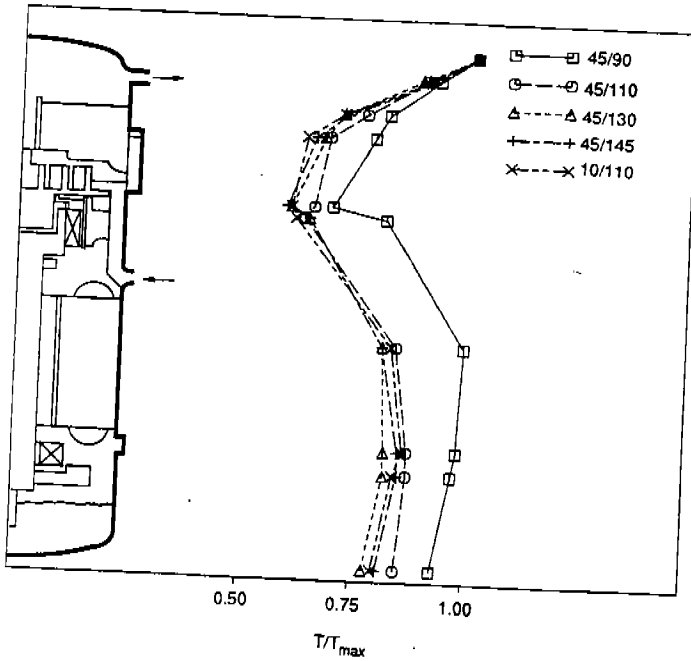
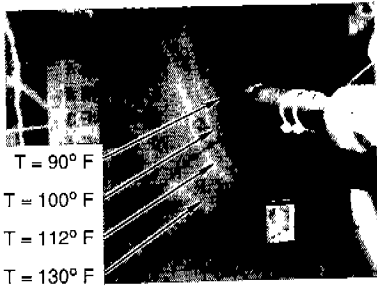
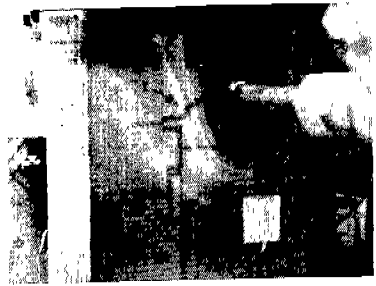


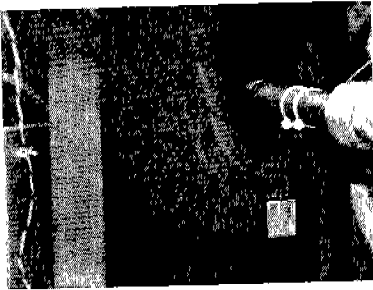
Fig. 4. Average shell temperature profiles



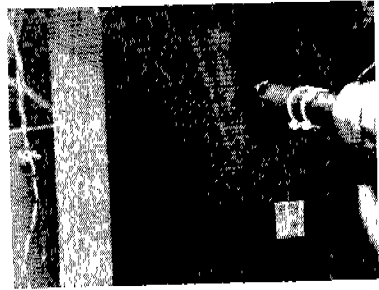
(a) 45/90



(b) 45/100



(c) 45/130



(d) 45/145

Fig. 5. Shell temperature contours

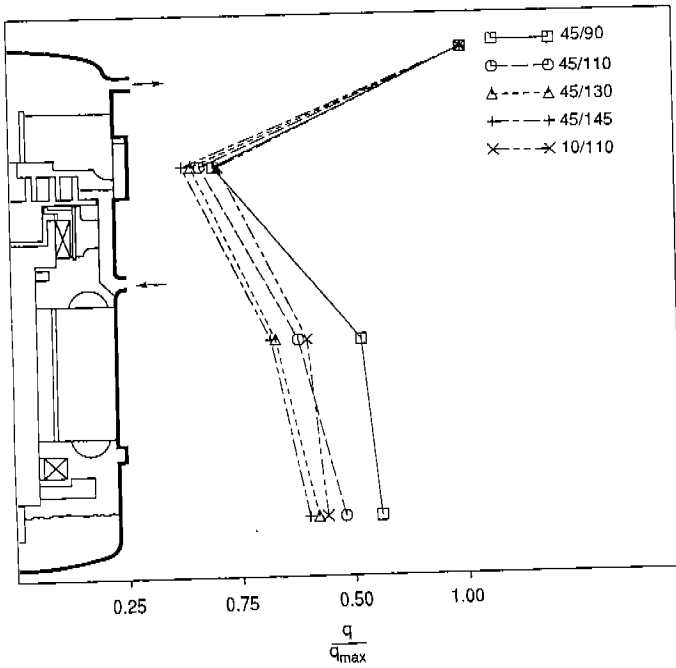


Fig. 6. Shell heat flux data

SATURATED EVAPORATING TEMPERATURE = 45° F

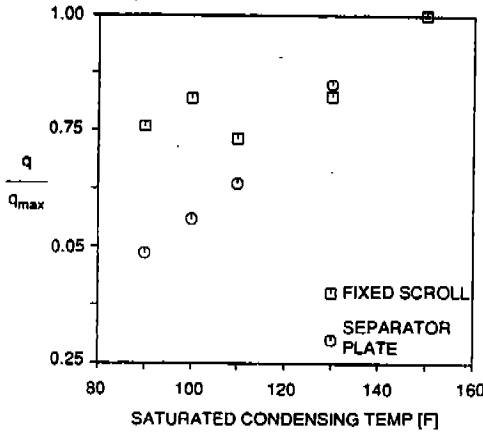


Fig. 7. Heat flux from fixed scroll and separator plate

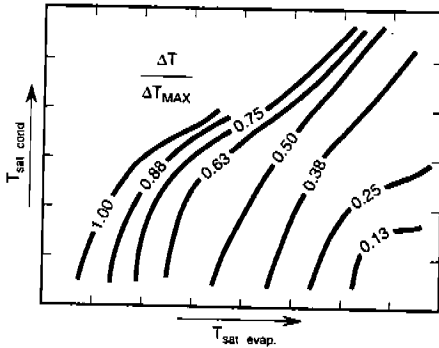


Fig. 8. Suction duct temperature rise

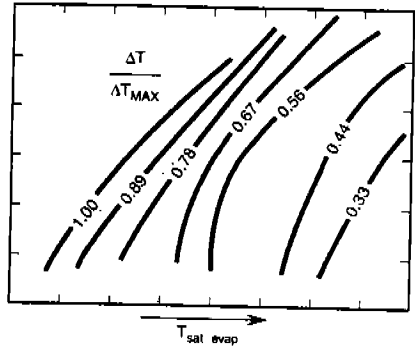


Fig. 9. Total suction gas temperature rise

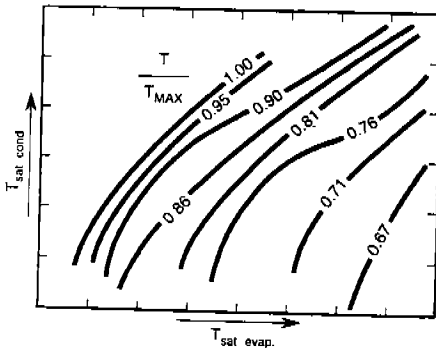


Fig. 10. Oil temperature

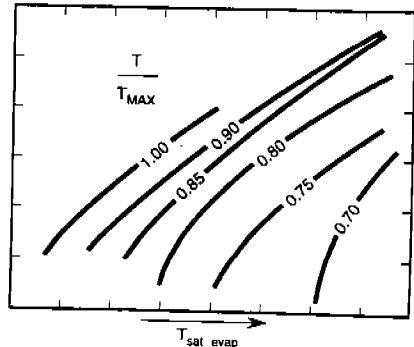


Fig. 11. Main bearing temperature

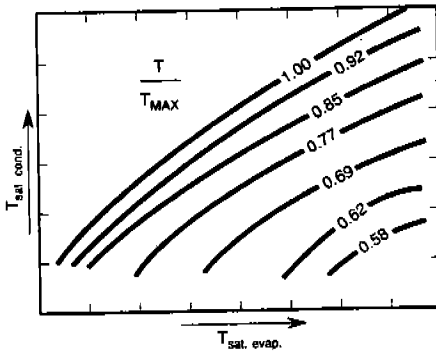


Fig. 12. Discharge temperature

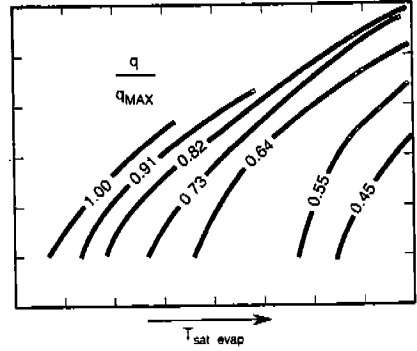


Fig. 13. Center shell heat flux

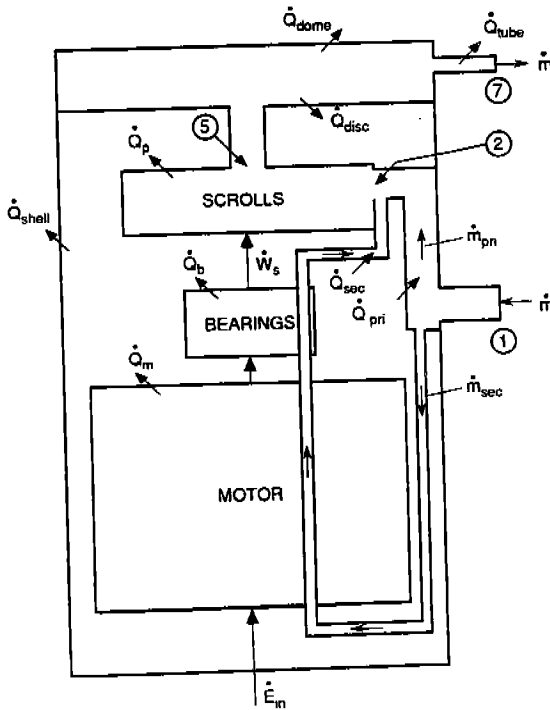


Fig. 14. Schematic diagram of scroll compressor model